Indoor GPS with Centimeter Accuracy using WiFi

Chen Chen*†, Yi Han*†, Yan Chen‡†, and K. J. Ray Liu*†
* University of Maryland College Park, College Park, MD 20742, USA
† Origin Wireless, Suite 1070, 7500 Greenway Center Drive, MD 20770, USA
‡ University of Electronic Science and Technology of China, Chengdu, Sichuan, China
E-mail: {cc8834, yhan1990, kjrliu}@umd.edu, eecyan@uestc.edu.cn

***Abstract*—Indoor positioning systems are drawing ascending attention from the academia as well as industry, motivated by a wide variety of indoor location-based services. Among the existing indoor positioning systems, WiFi-based schemes are more favorable because of the ubiquitous WiFi infrastructures. However, both strong non-line-of-sight scenario and severe ambiguity among location-specific fingerprints prevent most existing WiFi-based indoor positioning systems from achieving centimeter accuracy for localization. In this paper, we propose an indoor positioning system which achieves centimeter accuracy and maintains the performance under non-line-of-sight scenarios using a single pair of off-the-shelf WiFi devices. By harvesting the inherent diversity in WiFi systems, the proposed indoor positioning system formulates a large effective bandwidth to provide a fine-grained location-specific fingerprint with a much higher resolution compared with the fingerprints in most WiFi-based indoor positioning systems. Extensive experiment results in a typical indoor environment show that the centimeter accuracy as well as robustness against environment dynamics can be achieved simultaneously with a large effective bandwidth.**

I. Introduction

The Global Positioning System (GPS) is a space-based navigation system that can provide location and time information whenever there is an unobstructed line-of-sight (LOS) path to four or more GPS satellites [1]. Such a system provides critical capabilities to military, civil and commercial applications around the world. On the other hand, considering the fact that people nowadays spend more than 80% of their time in indoor environments, accurate indoor localization is highly desirable and has great potential impact on many applications. Unfortunately, the use of GPS satellites to enable indoor localization is a non-starter due to a variety of reasons including poor signal strength, multipath effect and limited on-device computation and communication power [2]. Therefore, over the past two decades, the research community has been urgently seeking new technologies that can enable high accuracy indoor localization. However, the results are still mostly unsatisfied. Microsoft hosted Indoor Localization Competitions in recent years and concluded that "The Indoor Location Problem is NOT Solved" [3].

Many indoor positioning systems (IPSs) have been developed by leveraging radio wave, magnetic field, acoustic signal, or other sensory information collected by mobile devices [4]. Most of these systems are based on the ranging technique. Ranging is a process to determine the distance from one location to another location by utilizing the collected information such as the received signal strength indicator (RSSI) and/or time of arrival (TOA). Typically, these systems require multiple anchors at known locations and dedicated devices to collect fine-grained information for accurate ranging.

Technology	Existing Hardware?	Min # anchors	Low Cost?	Res. (m) LOS	Res. (m) NLOS	Commercial Examples
RSSI	✓	3	—	1-3	5-10	Active RFID, iBeacon, SPIRIT Navigation, Modulated LEDs
TOA TDOA	✗	3	✗	0.2-0.4	1-5	UWB, Decawave, Time Domain, Zebra, Nanotron
AOA	✓	2	—	0.4	1-5	None
Time Reversal	✓	1	✓	0.02	0.02	Origin Wireless

Fig. 1: State-of-the-art indoor positioning systems.

However, when there exist obstacles between the localized device and the anchors, the localization performance degrades significantly. In other words, the ranging-based systems cannot maintain highly accurate localization performance under non-line-of-sight (NLOS) scenarios, which is very common in the indoor environment. The performance degradation is fundamentally due to that the physical ranging rules that translate the collected information into distance are impaired by the blockage and multipaths naturally existing in the indoor environment. Developing a general physical ranging rule that suits for NLOS conditions is practically difficult, if not impossible, due to the complicated indoor environment, which motivates the development of the fingerprint-based IPSs. A summary of the existing state-of-the-art capabilities from the Microsoft hosted Indoor Localization Competitions is given in Fig. 1, in which one can see that under the LOS condition, with more than one anchors, sub-meter accuracy can be achieved. However, under the NLOS condition, only the meter-range can be obtained by most methods, except the recently proposed time-reversal approach that can obtain $1-2$ cm accuracy for both LOS and NLOS conditions [5].

In an indoor environment, there naturally exists some location-specific information, known as the fingerprint. Examples include magnetic field, RSSI, and channel state information (CSI). All these fingerprints can be exploited for indoor localization. Specifically, in the fingerprint-based IPS, the location-specific fingerprints are collected and stored into a database in the mapping phase. Then, in the localization phase, the location of the device is determined by comparing the device fingerprint with those in the database. In [5], it was shown that the physical phenomenon of time-reversal focusing effect can provide a high-resolution fingerprint for

indoor localization. The authors used a dedicated device to obtain the channel impulse response under the 5 GHz ISM band with a bandwidth of 125 MHz as the fingerprint, and utilized the time-reversal resonating strength (TRRS) as the similarity measure, which gives an accuracy of $1-2$ cm.

The question now is: can one use the ubiquitous WiFi devices to achieve the same? The answer is yes as evidenced from the recent works in [6]–[8]. The work in [6], [7] leveraged frequency hopping, while the work in [8] used multi-antenna spatial diversity to increase the effective bandwidth. As a result, the localization resolution can be significantly improved to $1-2$ cm.

This paper will enlighten the basic principles of how one can achieve indoor locationing resolution down to centimeter accuracy level using standard WiFi devices. A unified view by combining both the frequency and spatial diversities is also presented.

II. How bandwidth affects the localization performance?

The main reason that most of fingerprint-based methods utilizing CSI in WiFi systems cannot achieve centimeter localization accuracy is due to the bandwidth limitation. More specifically, the maximum bandwidth in mainstream WiFi devices is only either 20 MHz or 40 MHz, which introduces severe ambiguity into the fingerprints of different locations and thus leads to the poor accuracy for indoor localization.

To clearly illustrate the impact of bandwidth on localization performance, we have conducted experiments to collect CSIs under different bandwidths in a typical indoor environment. Two channel sounders are placed in an NLOS setting, where one of them is placed on a customized experiment structure with 5mm resolution.

To characterize the similarity between CSIs collected at different locations, the TRRS is calculated as

$$\gamma[\mathbf{H},\mathbf{H}'] = \left(\frac{\eta}{\sqrt{\Lambda}\sqrt{\Lambda'}}\right)^2, \tag{1}$$

with

$$\eta = \max_{\phi}\left|\sum_{k=1}^{K} H_k H_k'^{*} e^{-jk\phi}\right|, \Lambda = \sum_{k=1}^{K}|H_k|^2, \Lambda' = \sum_{k=1}^{K}|H_k'|^2, \tag{2}$$

where $\mathbf{H}$ and $\mathbf{H}'$ represent two fingerprints, K is the total number of usable subcarriers, H_k and H_k' are the CSIs on subcarrier k, η is the modified cross-correlation between $\mathbf{H}$ and $\mathbf{H}'$ with synchronization error compensation, and Λ, Λ' are the channel energies of $\mathbf{H}$ and $\mathbf{H}'$, respectively. Realizing that the WiFi receiver may not be fully synchronous with the WiFi transmitter due to mismatches in their radio-frequency front-end components [9], an additional phase rotation of $e^{-jk\phi}$ is employed to counteract the phase distortions incurred by the synchronization errors in the calculation of η. Eqn. (1) implies that TRRS ranges from 0 to 1. More specifically, a larger TRRS indicates a higher similarity between two fingerprints and thus the two associated locations.

The corresponding TRRS between the target location and nearby locations are illustrated in Fig. 2 under different bandwidth settings. It is shown in Fig. 2(a) that with 40 MHz bandwidth, a large region of nearby locations is ambiguous with the target location in terms of the TRRS. Enlarging the bandwidth shrinks down the area of ambiguous regions. As demonstrated in Fig. 2(c), when the bandwidth increases to 360 MHz, the ambiguous region is reduced to a ball of 1 cm in radius which implies centimeter accuracy in localization.

The experiment results motivate us to formulate a large effective bandwidth by exploiting diversities on WiFi devices to facilitate centimeter accuracy indoor localization.

III. Increasing Effective Bandwidth via Diversity Exploitation

Two different diversities exist in current WiFi system, i.e., frequency diversity and spatial diversity. According to IEEE 802.11n, 35 channels differing in center frequencies are dedicated for WiFi systems in 2.4 GHz and 5 GHz frequency bands, with a maximum bandwidth of 40 MHz for each channel. The multitude of WiFi channels leads to frequency diversity in that, they provides opportunities for WiFi devices to perform frequency hopping when experiencing deep fading or severe interference. On the other hand, spatial diversity can be exploited on multiple-input-multiple-out (MIMO) WiFi devices, which is a mature technique that significantly boosts the spectral efficiency. MIMO has not only become an essential component of IEEE 802.11n/ac, but also been ubiquitously deployed on numerous commercial WiFi devices. For WiFi systems, both types of diversity can be harvested to provide fingerprint with much finer granularity and thus less ambiguity in comparison with the fingerprint measured with a bandwidth of only 40 MHz.

For a WiFi system, the spatial diversity is determined by the number of antenna links, denoted as S, while the frequency diversity is dependent on the number of WiFi channels, denoted as F. Assume that the bandwidth for each WiFi channel is W, the effective bandwidth can be calculated as $S \times F \times W$.

IV. Achieving Centimeter Accuracy via Time-Reversal Resonating Strength

A. Calculating Time-Reversal Resonating Strength by Diversity Exploitation

As discussed in Section II and III, in order to achieve centimeter localization accuracy, a large effective bandwidth beyond 40 MHz is required, which can be obtained by diversity exploitation. For WiFi devices with a spatial diversity of S and a frequency diversity of F, the CSI measurements can be written as $\overline{\mathbf{H}} = \{\mathbf{H}_{s,f}\}_{s=1,2,\cdots,S}^{f=1,2,\cdots,F}$, where $\mathbf{H}_{s,f}$ stands for the CSI measured with the s-th antenna link on the f-th WiFi channel, denoted as the virtual link (s,f). $\overline{\mathbf{H}} = \{\mathbf{H}_{s,f}\}_{s=1,2,\cdots,S}^{f=1,2,\cdots,F}$ can provide fine-grained fingerprint with an effective bandwidth of $S \times F \times W$. Consequently, TRRS in (1) can be extended to the fine-grained fingerprint $\overline{\mathbf{H}}$ and $\overline{\mathbf{H}'}$, with

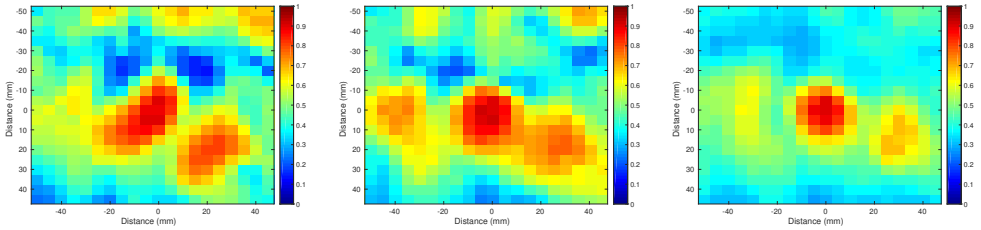

(a) 40 MHz Bandwidth (b) 120 MHz Bandwidth (c) 360 MHz Bandwidth

Fig. 2: Ambiguity with nearby locations under different bandwidths.

η and Λ, Λ' modified as

$$\eta = \sum_{s=1}^{S}\sum_{f=1}^{F}\eta_{s,f},\ \Lambda = \sum_{s=1}^{S}\sum_{f=1}^{F}\Lambda_{s,f},\ \Lambda' = \sum_{s=1}^{S}\sum_{f=1}^{F}\Lambda'_{s,f}\ , \tag{3}$$

where

$$\eta_{s,f} = \max_{\phi}\left|\sum_{k=1}^{K} H_{s,f,k}H'^{*}_{s,f,k}e^{-jk\phi}\right| \tag{4}$$

represents the modified cross-correlation on the virtual link (s,f), and $\Lambda_{s,f} = \sum_{k=1}^{K}|H_{s,f,k}|^2$, $\Lambda'_{s,f} = \sum_{k=1}^{K}|H'_{s,f,k}|^2$ are the channel energies of $\mathbf{H}_{s,f}$ and $\mathbf{H}'_{s,f}$ on the virtual link (s,f), respectively. The combined TRRS is calculated the same as (1).

B. Localization using Time-Reversal Resonating Strength

There are two phases in the proposed IPS: a mapping phase and a localization phase. During the mapping phase, the CSIs are collected from L locations-of-interest using WiFi devices with S antenna links and across F WiFi channels, denoted by $\left\{\overline{\mathbf{H}}_\ell\right\}_{\ell=1,2,\cdots,L}$. In the localization phase, $\overline{\mathbf{H}'}$ is obtained at a testing location, which may either be one of the L locations-of-interest or an unmapped location in the mapping phase. Then, the pairwise TRRS $\gamma[\overline{\mathbf{H}}_\ell, \overline{\mathbf{H}'}]$ is calculated for all locations-of-interest. Finally, the location is determined based on $\gamma[\overline{\mathbf{H}}_\ell, \overline{\mathbf{H}'}]$, i.e,

$$\hat{\ell} = \begin{cases} \underset{\ell=1,2,\cdots,L}{\operatorname{argmax}}\ \gamma[\overline{\mathbf{H}}_\ell, \overline{\mathbf{H}'}], & \max\limits_{\ell=1,2,\cdots,L}\gamma[\overline{\mathbf{H}}_\ell, \overline{\mathbf{H}'}] \geq \Gamma \\ 0, & \text{Otherwise} \end{cases} \tag{5}$$

where Γ is a threshold introduced to balance off the true positive rate and false positive rate in location determination. When $\gamma[\overline{\mathbf{H}}_\ell, \overline{\mathbf{H}'}]$ falls below Γ, the IPS cannot obtain a credible location estimation and returns 0 to imply an unmapped location.

V. Experiment Results

Extensive experiments are conducted to validate the theoretical analysis and evaluate performance of proposed IPS. The proposed system contains two WiFi devices, each equipped with three antennas. One WiFi device, called Origin, estimates CSI from the other WiFi device, named as Bot. With the proposed algorithm in Section IV, Origin estimates the location of Bot.

The experiments are conducted in a typical office of a multi-storey building. The indoor space is filled with a large number of reflectors, e.g., chairs, desks, shelves, sofas, walls, and ceilings. The CSIs of 50 candidate locations are measured, with 20 measurements for each location.

To evaluate the performance, the CSIs at each location are partitioned into a training set and a testing set, with 10 CSIs for each. The TRRS matrix is calculated using the CSIs collected at the 50 candidate locations. Each element of the matrix represents the TRRS between the CSIs at the training location and the testing location. In other words, the diagonal elements of matrix indicate the similarity between CSIs at the same location, while the off-diagonal elements stand for the similarity between CSIs of different locations.

Fig. 3 illustrates the TRRS matrices under effective bandwidths of 10, 40, 120, and 360 MHz. First of all, it is easily seen from Fig. 3 that the diagonal elements of the matrices are close to 1, signifying high similarities among CSIs of the same locations. Regarding the off-diagonal elements, they become smaller with an increasing effective bandwidth. When the effective bandwidth is small, e.g., 10 MHz, some off-diagonal elements are even larger than the diagonal elements, giving rise to localization errors. In other words, it is very likely to localize the Bot to incorrect positions when the effective bandwidth is small. When the effective bandwidth is increased, the gap between diagonal and off-diagonal elements enlarges, which provides a clear watershed between the correct and incorrect locations, leading to an enhanced system performance in return.

To provide a statistical point of view, Fig. 4 shows the cumulative density functions (CDF) of the diagonal and off-diagonal elements in TRRS matrices under a variety of effective bandwidths. As we can see, the gap between the diagonal and off-diagonal elements increases with the effective bandwidth, indicating a better distinction between different locations. Whenever there is a gap between the diagonal and off-diagonal elements, a perfect localization can be achieved with an appropriate threshold, i.e., 100% true positive rate and 0% false positive rate.

In a practical indoor environment, there usually exists environment dynamics that might degrade the localization performance. To evaluate the proposed IPS in a dynamic indoor environment, the testing CSIs are re-collected in the presence of human activities and large object movement. In

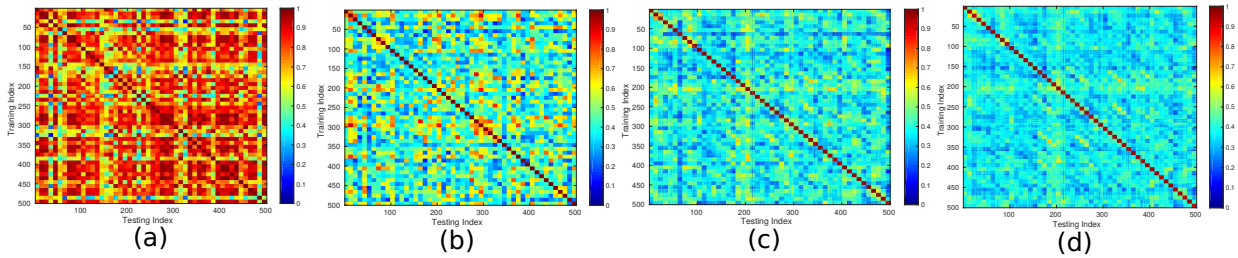

Fig. 3: TRRS matrix under an effective bandwidth of (a) 10 MHz (b) 40 MHz (c) 120 MHz (d) 360 MHz.

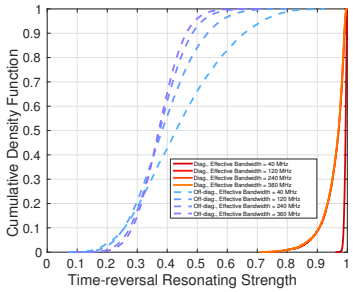

Fig. 4: CDF of the TRRS of the diagonal and off-diagonal elements.

particular, to emulate dynamics from human activities, one participant was asked to walk continuously in the vicinity of the Bot. Then, the participant was asked to open and close a door which blocks the direct link between the Origin and Bot so as to emulate the dynamics from large object movement.

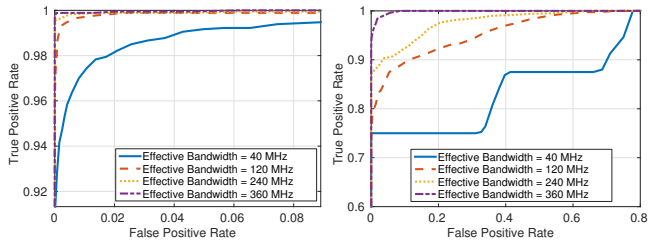

Fig. 5: ROC curve with dynamics. (a) Dynamics from human movement. (b) Dynamics from large object movement.

Fig. 5(a) demonstrates the receiver operating characteristic (ROC) curve with human acitivities. For a fixed false positive rate 0.15%, the true positive rate increases from 94.17% with 40 MHz effective bandwidth to 99.11% with 120 MHz effective bandwidth. Further enlarging the effective bandwidth to 240 MHz and 360 MHz boosts the true positive rate to 99.61% and 99.89%, respectively. On the other hand, Fig. 5(b) depicts the ROC curve with large object movement. For a fixed false positive rate 0.15%, the true positive rate increases from 75% with 40 MHz effective bandwidth to $76.38\%, 87.12\%$, and 95% with $120, 240$, and 360 MHz effective bandwidths, respectively. This can be justified by that with a large effective bandwidth, the environment dynamics only affect very limited information in the fingerprint while leaving majority of the fingerprint intact. In other words, a large effective bandwidth enhances the robustness of the proposed IPS against environment dynamics.

VI. Conclusion

In this paper, we present a time-reversal method for indoor localization that achieves centimeter accuracy with a single-pair of off-the-shelf WiFi devices. The high accuracy for localization is maintained under strong NLOS scenarios. With the exploitation of the inherent frequency and spatial diversities in WiFi systems, it is capable of creating a large effective bandwidth to enable centimeter accuracy. Extensive experiment results in a typical office environment shows that the centimeter accuracy as well as robustness against dynamics can be simultaneously achieved with a large effective bandwidth. The global GPS can achieve $3-15$ meter of accuracy by mapping the world into latitude and longitude coordinates. The presented "indoor GPS" can achieve $1-2$ cm accuracy when an indoor environment is fingerprinted and mapped.

References

[1] J. G. McNeff, "The global positioning system," *IEEE Transactions on Microwave Theory and Techniques*, vol. 50, pp. 645–652, March 2002.

[2] S. Nirjon, J. Liu, G. DeJean, B. Priyantha, Y. Jin, and T. Hart, "Coin-GPS: indoor localization from direct GPS receiving," in *Proceedings of the 12th annual international conference on Mobile systems, applications, and services*, pp. 301–314, ACM, 2014.

[3] Microsoft, "Microsoft indoor localization competition – IPSN 2016." http://research.microsoft.com/en-us/events/msindoorloccompetition2016/, April 2016.

[4] K. Curran, E. Furey, T. Lunney, J. Santos, D. Woods, and A. McCaughey, "An evaluation of indoor location determination technologies," *Journal of Location Based Services*, vol. 5, no. 2, pp. 61–78, 2011.

[5] Z.-H. Wu, Y. Han, Y. Chen, and K. J. R. Liu, "A time-reversal paradigm for indoor positioning system," *IEEE Trans. Veh. Technol.*, vol. 64, no. 4, pp. 1331–1339, 2015.

[6] C. Chen, Y. Chen, H. Q. Lai, Y. Han, and K. J. R. Liu, "High accuracy indoor localization: a WiFi-based approach," in *2016 IEEE International Conference on Acoustics, Speech and Signal Processing (ICASSP)*, pp. 6245–6249, March 2016.

[7] C. Chen, Y. Chen, Y. Han, H. Lai, and K. J. R. Liu, "Achieving centimeter accuracy indoor localization on single-antenna WiFi platforms," *IEEE SigPort*, June 2016. http://sigport.org/1119.

[8] C. Chen, Y. Chen, Y. Han, H. Lai, F. Zhang, and K. J. R. Liu, "Achieving centimeter accuracy indoor localization on multi-antenna WiFi platforms," *IEEE SigPort*, June 2016. http://sigport.org/1118.

[9] M. Speth, S. Fechtel, G. Fock, and H. Meyr, "Optimum receiver design for wireless broad-band systems using OFDM—Part I," *IEEE Trans. Commun.*, vol. 47, pp. 1668–1677, Nov. 1999.